Biogeosciences Discuss., 5, 3945–3964, 2008
www.biogeosciences-discuss.net/5/3945/2008/

Biogeosciences Discussions

Biogeosciences Discussions is the access reviewed discussion forum of *Biogeosciences*

CO_2 radiative forcing during the Holocene Thermal Maximum revealed by stomatal frequency of Iberian oak leaves

I. García-Amorena[1], F. Wagner-Cremer[2], F. Gomez Manzaneque[1], T. B. van Hoof[3], S. García Álvarez[1], and H. Visscher[2]

[1]Unidad Docente de Botanica, Escuela Técnica Superior de Ingenieros de Montes, Universidad Politécnica de Madrid, Madrid, Spain
[2]Palaeoecology, Laboratory of Palaeobotany and Palynology, Faculty of Sciences, Utrecht University, Utrecht, The Netherlands
[3]TNO Geological Survey of the Netherlands, Utrecht, The Netherlands

Received: 27 August 2008 – Accepted: 27 August 2008 – Published: 2 October 2008

Correspondence to: I. García-Amorena (ignacio.garciaamorena@upm.es)

Published by Copernicus Publications on behalf of the European Geosciences Union.

Abstract

Here we analyse radiocarbon-dated *Quercus* leaf assemblages from northern Spain to obtain past atmospheric CO_2 mixing ratios for the time period 9000–1100 cal BP by means of stomatal frequency analysis. Normalized, stomata based CO_2 records show fluctuations of 20 ppmv during the Holocene that parallel Northern Hemisphere palaeotemperature reconstructions. The calculated radiative forcing of CO_2 indicates a CO_2 contribution of +0.1°C to the Holocene Thermal Maximum from 7 to 5 kyr BP, and −0.05°C to the Neoglacial cooling around 4 kyr BP. Derived northern hemispheric air-temperature anomalies forced by atmospheric CO_2 variation suggest an active role of this trace gas as an amplifier of initial orbital forcing of Holocene climate.

1 Introduction

Earth's orbital variation is considered the fundamental cause of climate change during the Holocene through precession and obliquity changes that drove the northern hemispheric (NH) insolation decrease during this period (Crucifix et al., 2002). However, insolation changes cannot completely explain the millennial scale climate evolution from the Holocene Thermal Maximum (HTM) to the Neoglaciation (Kaufman et al., 2004) observed in an extensive number of mid- to late-Holocene terrestrial and marine records in the Northern Hemisphere (Marchal et al., 2002; Seppä et al., 2005; Ojala et al., 2008). Internal feedback mechanisms of the climate system that may have contributed to the climate evolution of the Holocene are not yet understood and often controversial.

With complex links to various parts of the climate system, changing atmospheric CO_2 remains one of the most important driving force behind climate change (Raynaud et al., 1993). However, the Antarctic ice core CO_2 records for the last 10 000 years show little CO_2 trace gas variation during the Holocene. A continuous CO_2 increase after minimum values around 8000 cal BP to pre-industrial times (Monnin et al., 2004; Indermühle et al., 1999) does not support a role of this trace gas in millennial-scale

mid- to late-Holocene climate evolution.

In contrast, atmospheric CO_2 reconstructions based on stomatal frequency analysis of common tree species detected a close link between global temperature and atmospheric CO_2 concentrations on centennial to decades time scales throughout the Holocene (van Hoof et al., 2005; Kouwenberg et al., 2005; Wagner et al., 2004; Jessen et al., 2005). The majority of these studies however focus on high resolution reconstructions of century-scale climate oscillations and only one record spanning major parts of the Holocene with highest data coverage from 5000 cal BP onwards is available so far (Rundgren and Björck, 2003). Although some features of this record are in agreement with the ice based CO_2 record for the Holocene, large discrepancies remain in the amplitude and magnitude of the reconstructed CO_2 levels. The high variability in the data set and the relatively low data coverage during the early- to mid-Holocene hamper a detailed analysis of the potential role of CO_2 during this period.

Here we present a stomatal based CO_2 record from well-preserved fossil *Q. robur* leaf assemblages, recovered from road cuts and sea-eroded cliffs in northern Spain. The multiple site study covers the early- to mid-Holocene, with one additional point in the late Holocene.

From the calculated radiative forcing of the reconstructed CO_2 fluctuations between 9000 cal BP and 1000 cal BP, potential temperature anomalies are derived. This procedure enables a direct comparison with existing proxy-based NH temperature records and allows an evaluation of the potential role of CO_2 as amplifying mechanism of insolation induced temperature anomalies observed throughout the Holocene.

2 Study area

Holocene leaf assemblages were collected at three locations, Villaviciosa, Pravia and Merón, located on the Cantabrian coast of the Iberian Peninsula (Fig. 1, Table 1). The Villaviciosa and Pravia estuaries are narrow incisions on a Jurassic basement filled by fluvial-marine Holocene sediments. The Villaviciosa lithology changes from gravels at

the basements to sandy matrix with rich organic matter intercalations, silty clays with plant remains and podzol with roots at the top. These successions are shown to correspond to high energy fluvial channels, intertidal flats and marshes, and recent forest soil, respectively (Pagés et al., 2003). The sixteen available cores drilled in Pravia show a similar stratigraphic pattern to the Villaviciosa estuary. In Villaviciosa, road works exposed more than 10 m deep outcrops, allowing 200 m cross section sampling. Leaves and other plant macro-remains were in situ collected in 2003. At the Pravia site, rich fossil leaf assemblages from various depths were recovered from two cores from the Cantabrian motorway pillar-basements drilling in 2005.

At the third sampling site, Merón (Fig. 1), peat deposits and clay sediments with plant remains are exposed in an eroded cliff section, that are infills of a hydrologic incision in the Pleistocene beach basement. The abundant plant remains, including rich leaf assemblages originate from the surrounding forests drowned during the Flandrian water table increase ~6000–7000 BP (Garzón et al., 1996).

3 Methods

The age assessment for the nine studied leaf assemblages is based on conventional ^{14}C dating of fossil wood collected from each layer or core sampled, undertaken by Beta Analytic Inc. (Miami, USA). Conventional radiocarbon ages were converted into cal BP using Oxcal 3.10 software (Bronk Ramsey, 2005) and employing a dendrochronological database (Reimer et al., 2004).

All sediment samples were sieved with 50 g/l tetra-sodium pyrophosphate ($Na_4P_2O_7$ $10H_2O$) to dilute the clay. *Q. robur* leaf fragments were extracted and identified by the morphological and anatomical characters (Castroviejo et al., 1986–2004; Westerkamp and Demmelmeyer, 1997). To exclude leaf fragments from hybrids with other *Quercus* species, only leaf remains with simple glandulate trichomes were analysed (Peñas et al., 1994; Uzunova et al., 1997). *Q. robur* leaf fragments were carefully brushed and, where necessary, immersed in 50% fluoric acid (HF) to remove remaining silica.

Samples of approximately 5×5 mm from the central part of the leaves, where stomatal and epidermal parameters are more stable (Poole et al., 1996), were bleached in 4% sodium hypochlorite (NaH ClO_2) for 30 s. After rinsing them for 5 min, they were mounted on microscopic slides with glycerine jelly to be measured on a Leica Quantimet 500C/500+Image Analysis System.

Ten leaf fragments of each horizon were taken to obtain stomatal and epidermal cell parameters as described in García-Amorena et al. (2006). On each leaf fragment stomatal density (SD [mm^{-2}]) and epidermal cell density (ED [mm^{-2}]) were measured on ten different and randomised areas of 0.0245 mm^2 within the alveoles. For the stomatal length (SL [μm]), pore length (PL [μm]), epidermal cell circumference (CC [μm]) and epidermal cell area (CA [μm^2]) measurements, ten different stomata or epidermal cells per leaf fragment were randomly selected. From the measured parameters, the stomatal index [SI [%]=100×SD/(SD+ED); Salisbury, 1927] and undulation index [UI=CC/$2\pi\sqrt{}$(CA/π); Kürschner, 1997] were calculated.

All measurements were made on sun morphotypes to avoid the effect of canopy variations in light, humidity and CO_2 on the leaf morphology (Lockheart et al., 1998; Bazzaz and Williams, 1991; Kürschner, 1996; Poole et al., 1996); sun leaves were determined by the periclinal wall undulation analysis (UI<1.5) (García-Amorena et al., 2006; Kürschner, 1997).

Atmospheric CO_2 concentrations (ppmv) were calculated for each sample by converting the SI average and 1×standard deviation with the CO_2 inference model [CO_2[ppmv]=−6.25×(SI-71.09); Garcia-Amorena et al., 2006], specifically developed for *Q. robur* grown within the range of 0 to 1000 m a.s.l. in mid- to low-latitudes. Variation in radiative forcing (dF [W/m^2]) induced by the inferred CO_2 shifts were calculated from the following approach proposed by Myhre et al. (1998):

$$dF = \alpha \cdot \ln\left[\frac{C}{CO}\right]$$

Where α=5.35, CO represents the unperturbed CO_2 base level of 278 ppmv as recommended by the IPCC (2001), and C is the CO_2 mixing radios (ppmv) here taken as

the reconstructed normalised CO_2 superimposed to the 278 ppmv base level.

The global temperature response to the calculated variations in radiative forcing were assessed based on calculations derived from the coupled ocean-atmospheric climate model; ECBilt-CLIO (Goosse and Fichefet, 1999; Opsteegh et al., 1998).

4 Results

^{14}C age assessments show that the Villaviciosa estuary records a large part of the Holocene, and is complimented by Merón and Pravia older Holocene sediments (Table 1). The collected fossil leaf assemblages accordingly cover the time period from 9300 to 1130 cal BP.

The measured SI data are shown in Fig. 2a, from which the atmospheric CO_2 mixing ratios were inferred (Table 1). Early Holocene values are characterized by high SI averages of 19.5% to 19.2%. A continuous SI decrease reaches a minimum of mean 16.4% (342 ppmv CO_2) at 5860 cal BP. Following a SI rise to 19% (326 ppmv CO_2) at 4110 cal BP, SI decreases to mean 17.9% (333 ppmv CO_2) at 3950 cal BP. Measured SI shows similar values of 17.8% (333 ppmv CO_2) at 1130 cal BP.

Reconstructed CO_2 levels are normalized in Fig. 2b in order to facilitate comparison of trends in atmospheric CO_2 observed in CO_2 records based on other reconstruction techniques and to calculate radiative forcing trends. A −9 ppmv deviation from the Holocene mean CO_2 value is observed at the early Holocene (9300 cal BP), steady rising to −4.1 ppmv at 7420 cal BP. From this date, the atmospheric CO_2 rises to up to 10.4 ppmv above the Holocene mean at 5860 cal BP, from which it follows a steeply decrease to reach −5.5 ppmv at 4110 cal BP from which CO_2 averages the Holocene mean values.

Radiative forcing variations induced by the SI inferred CO_2 concentrations are plotted in Fig. 3a. The CO_2 concentration changes throughout the Holocene explain up to 0.19°C Northern Hemisphere temperature variation between the CO_2 minimum at 9300 cal BP and the Holocene maximum at 5860 cal BP (Fig. 3b). 0.15°C difference is

observed in this figure between the Holocene CO_2 peak value to a second minimum at 4110 cal BP.

5 Discussion

5.1 Holocene CO_2 reconstruction

The CO_2 estimates based on Spanish *Quercus robur* leaf assemblages indicate CO_2 concentrations on relatively high levels, with a mean of 320 ppmv for all samples analysed. This high baseline is a so far unexplained feature common to all reconstructions based on stomatal frequency, independent of geographical origin of the leaf material or genus studied (Wagner et al., 1999, 2002; Rundgren and Beerling, 1999; McElwain et al., 2002; Kouwenberg et al., 2003; Jessen et al., 2007). The reconstructed CO_2 concentrations for the mid-Holocene however, equal the levels detected in the Swedish Lake Njulla record (Rundgren and Beerling, 1999). In contrast to the former study however, where for the mid-Holocene up to 100 ppmv variability are present in the raw data, our record follows a successive trend, that indicates gradual changes in the Holocene CO_2 regime.

Despite the remaining uncertainties in terms of CO_2 base-level, normalized stomatal frequency based CO_2 records have been demonstrated to capture amplitude changes in CO_2 that can be lost in ice core CO_2 records due to smoothing of the gas concentration in air bubbles during the firn densification process (Trudinger et al., 2003; van Hoof et al., 2005).

The most prominent feature in the normalized stomatal index based CO_2 reconstruction is the phase of elevated CO_2 between 7400 cal BP and 4100 cal BP, where CO_2 is up to 10 ppmv higher than the Holocene average. Although our record consists of only a rather small amount of data, the long-term trends are well revealed by the continuity of the changes reconstructed.

Comparing the data to Antarctic ice-core CO_2 profiles, the general trends during the

earlier Holocene are in good agreement, with low CO_2 levels around 8000 cal BP and a successive increase until approximately 6000 cal BP (Indermühle et al., 1999; Monnin et al., 2004). Although the trends are the same, the absolute CO_2 increase is 10 ppmv in Taylor Dome, and 14 ppmv in the stomata based record.

During the later part of the Holocene, the general patterns diverge. While in the Antarctic records CO_2 increases continuously by another 15 ppmv until 1000 cal BP, a drawdown of 10 ppmv CO_2 between 5800 cal BP and 4100 cal BP is documented in the stomata based record. The pronounced mid-Holocene maximum is followed by relatively stable values. Although the period from 4100 to 1100 cannot be interpreted in detail due to the very low data density in this part, the general trend from 5800 cal BP to 1100 cal BP indicates a downwards tendency rather than the continuous increase deduced from ice-cores.

On millennial time-scales, terrestrial biosphere and the oceans are the most likely sources and sinks for atmospheric carbon (Bacastow, 1996; Liu et al., 2003). The common to both records increase in CO_2 between 8000 cal BP and 6000 cal BP coincides well with the recovery from the 8.2 kyr cool pulse, where a weakening of the thermohaline circulation triggered by a catastrophic meltwater release lead to changes in sea-surface temperature and salinity (Alley et al., 1997). The presence of a CO_2 minimum around 8.2 kyrs is observed in ice-core data as well as in stomata based records (Rundgren and Beerling, 1999; Wagner et al., 2002, 2004) which fit well in, and close the data gap between 8500 cal BP and 7400 cal BP in our record. Considering the ocean properties as major constituent to CO_2 changes, the continuing increase in CO_2 indicated in ice-cores cannot be explained since it would require a warming of 2.3°C mean SST between 7000 cal BP and 1000 cal BP (Indermühle et al., 1999). No such Holocene SST increase is documented so far. On the contrary, recent reconstructions of SST over a wide geographical range postulate a widespread, long-term cooling of the sea surface associated with the transition from the Holocene Hypsithermal to the Neoglaciation (Marchal et al., 2002). Overall cooling of the ocean surface would potentially provide a significant sink for atmospheric carbon leading to the successive CO_2

decrease as observed in the stomata based record.

5.2 The role of CO_2 radiative forcing on Holocene climate change

The calculated radiative forcing for the CO_2 shifts reconstructed indicate with $-0.06\,W/m^2$ a negative deviation from Holocene average levels in the oldest part of the record, with a successive intensification to $+0.06\,W/m^2$ to 5800 cal BP, from where CO_2 forcing declines again to stabilize around Holocene mean values in the late Holocene. These changes can be translated in phases of temperature deviations, where atmospheric CO_2 radiative forcing contributes +0.1°C during the mid-Holocene and −0.05°C to +0.02°C in its continuation from 5800 cal BP to 1100 cal BP.

The pacing of the temperature shifts deduced from the CO_2 radiative forcing corresponds very well to known Holocene climate anomalies recorded in a wide variety of marine and terrestrial proxy records. Most striking is the parallelism of elevated temperature between 7400 cal BP and 5800 cal BP and the Holocene Thermal Maximum (HTM), concomitant to the positive CO_2 anomalies up to +10.4 ppmv from ∼7000 cal BP to ∼5000 cal BP (shades area in Fig. 3); and the Neoglacial cooling (NC) revealed by −5.5 ppmv CO_2 deviation at 4110 cal BP (Alley et al., 1997; Kaplan and Wolfe, 2006; Kaufman et al., 2004).

Correlations between stomata-based CO_2 records with existing local palaeotemperature reconstructions during the Holocene are generally hampered by different response times, sensitivity of individual records and spatial occurrence to climate variations (Kaufman et al., 2004). However, reconstructed summer temperature anomalies derived from pollen and chironomid assemblages in the northern Iberian Range (Peñalba et al., 1997) and in the northern Swiss Alps (Heiri et al., 2003) are both highly sensitive to regional temperature changes. These records correlate well with our derived radiative forcing fluctuations. The HTM peak is characterised in these records by +1.13 and +0.57°C deviation, and a −0.8/−0.51°C anomalies at the minimum NC are followed by an increase to −0.33 / −0.23°C at ∼1100 cal BP (Fig. 3c, d).

Mean annual temperature reconstructions from boreholes (Dahl-Jensen et al., 1998)

and spatially averaged Holocene temperature records for the NH (Kaufman et al., 2004) reveal the same temporal pattern of comparable shifts in temperature. Peak HTM is reached at 7 kyr BP in the majority of the records (Kaplan and Wolfe, 2006), with 1.6±0.8°C mean positive anomaly (Kaufman et al., 2004). In some records, these high temperatures are maintained for 2–3 kyr BP (Fig. 3e) (Dahl-Jensen et al., 1998). A steady temperature decrease following the HTM is observed in most of the NH palaeotemperature reconstructions (Fig. 3f) (Andersen et al., 2004; Kaplan and Wolfe, 2006). A pollen and chironomid based temperature decline is observed from the HTM to ∼4 kyr BP paralleling the stomatal CO_2 reconstruction (Figs. 2b, 3c, 3d). In the uppermost horizon studied, the temperature increase recorded in NH temperature reconstructions (Fig. 3) coincides with the return to Holocene mean CO_2 concentrations.

The strong link between the referred Holocene palaeotemperature reconstructions for the NH and our stomatal CO_2 data (Figs. 2, 3) suggest that the 20 ppmv CO_2 shifts observed for this period explain up to 0.2°C variation. The amplitude of this forcing is about 10% of the NH Holocene mean temperature anomalies.

Although it is agreed that climate is driven by Earth's orbital variation (Kaufman et al., 2004) the Holocene millennial-scale climatic shifts cannot solely be explained by the steady reduction of annual mean insolation during this time-period. For example, the $2\,W/m^2$ reductions at 65°N from 10 kyr BP to present could only explain 1°C reduction (Crucifix et al., 2002; Liu et al., 2003). Recent studies combining numerical climate models with palaeoenvironmental records attribute Holocene climate events to a range of forcing factors (e.g. Laurentide Ice Sheet albedo and melting, timing of plant colonization, atmospheric-ocean circulation) (Kaufman et al., 2004). Yet, although atmospheric trace gas concentrations have been considered in these studies, CO_2 concentrations have been disseminated due to the non-variability observed in the widely used Antarctic ice cores CO_2 reconstructions (Indermühle et al., 1999; Trudinger et al., 2003; van Hoof et al., 2005).

In contrast, the 0.2°C CO_2 radiative forcing, estimated by the stomatal based 20 ppmv CO_2 shifts throughout the Holocene, accounts for ∼20% of the variation in

annual insolation at 65° N. This highlights the magnitude of the atmospheric CO_2 forcing on the millennial time scale Holocene climate system.

Therefore, it can be hypothesized that the atmospheric CO_2 feedbacks and amplification of orbital forcing had a strong influence on millennial-scale Holocene climate. This is also supported by long term Quaternary CO_2-temperature coupling and model simulations on historical observations that indicated a positive feedback of CO_2 on temperature variations (Petit et al., 1999; Raynaud et al., 1993; Shackleton, 2000; Stott and Kettleborough, 2002).

6 Conclusions

The stomatal frequency based CO_2 record for the period from ∼9000 cal BP to ∼5000 cal BP shows for the comparable trends of continuously increasing CO_2 by approximately 10 ppmv as deduced from Antarctic ice cores. This CO_2 increase accounts for a temperature increase of +0.1°C. The positive temperature anomaly is concomitant with temperature rises evident from a wide variety of marine and terrestrial proxies and parallels the HTM.

From 5000 cal BP to ∼1100 cal BP, the CO_2 profiles from stomata and ice diverge. Where the ice record indicates a further gradual CO_2 increase to pre-industrial levels, the stomata records suggests a CO_2 decrease driving the temperature back by −0.05°C. Although this is in contrast to the evidence from Antarctic ice cores, the estimated temperature decline matches the majority of reconstructions for the second half of the Holocene, where after peak warmth during the HTM temperatures decrease again during the Neoglacial cooling.

Thus positive CO_2 feedbacks of orbital driven Holocene climate parallels the HTM warmth and neoglacial cooling. However, the different pattern observed between the CO_2 trend and the steady annual insolation decrease during the Holocene suggests orbital forcing independent mechanisms of CO_2 exchange to contribute to the millennial-scale Holocene climate shifts.

Acknowledgements. We thank M. Rundgren for his useful comments on the manuscript, the geologists M. Hacar and I. Martínez for help with sampling the road cuts before destruction. The material was sampled thanks to the collaboration of A. Alonso, J. L. Pagés (Universidad de La Coruña, Spain) and the Palaeobotany Research Group of the Universidad Politécnica de Madrid (Spain). This work has been supported by the projects CGL2004-00048/BT and CGL2006-0956/BOS (Ministerio de Ciencia y Tecnología, Spain). This paper is the Netherlands Research School of Sedimentary Geology Publication no. 20080903.

References

Alley, R. B., Mayewski, P. A., Sowers, T., Stuiver, M., Taylor, K. C., and Clark, P. U.: Holocene climatic instability: A prominent, widespread event 8200 yr ago, Geology, 25, 483–486, 1997.

Andersen, K. K., Azuma, N., Barnola, J. M., Bigler, M., Biscaye, P., Caillon, N., Chappellaz, J., Clausen, H. B., Dahl-Jensen, D., Fischer, H., Fluckiger, J., Fritzsche, D., Fujii, Y., Goto-Azuma, K., Gronvold, K., Gundestrup, N. S., Hansson, M., Huber, C., Hvidberg, C. S., Johnsen, S. J., Jonsell, U., Jouzel, J., Kipfstuhl, S., Landais, A., Leuenberger, M., Lorrain, R., Masson-Delmotte, V., Miller, H., Motoyama, H., Narita, H., Popp, T., Rasmussen, S. O., Raynaud, D., Rothlisberger, R., Ruth, U., Samyn, D., Schwander, J., Shoji, H., Siggard-Andersen, M. L., Steffensen, J. P., Stocker, T., Sveinbjornsdottir, A. E., Svensson, A., Takata, M., Tison, J. L., Thorsteinsson, T., Watanabe, O., Wilhelms, F., and White, J. W. C.: High-resolution record of Northern Hemisphere climate extending into the last interglacial period, Nature, 431, 147–151, 2004.

Bacastow, R. B.: The effect of temperature change of the warm surface waters of the oceans on atmospheric CO_2, Global Biogeochem. Cy., 10, 319–334, 1996.

Bazzaz, F. and Williams, W.: Atmospheric CO_2 concentrations within a mixed forest: implications for seedling growth, Ecology, 12, 12–16, 1991.

Bronk Ramsey, C.: OxCal progam v3. 10, available at: http://www.rlaha.ox.ac.uk/oxcal/oxcal.htm (last access: 26 March 2008), 2005.

Castroviejo, S., Laínz, M., López, G., Monserrat, P., Muñoz, F., Paiva, J., and Villar, L.: Flora ibérica. Plantas vasculares de la Península Ibérica e Islas Baleares, Real Jardín Botánico, C.S.I.C. Madrid, Madrid, Spain, 1986–2004.

Crucifix, M., Loutre, M. F., Tulkens, P., Fichefet, T., and Berger, A.: Climate evolution during the

Holocene: a study with an Earth system model of intermediate complexity, Clim. Dynam., 19, 43–60, 2002.
Dahl-Jensen, D., Mosegaard, K., Gundestrup, N., Clow, G. D., Johnsen, S. J., Hansen, A. W., and Balling, N.: Past Temperatures Directly from the Greenland Ice Sheet, Science, 282, 268–271, 1998.
García-Amorena, I., Wagner, F., van Hoof, T., and Gómez Manzaneque, F.: Stomatal responses in deciduous oaks from southern Europe to the anthropogenic atmospheric CO_2 increase; refining the stomatal-based CO_2 proxy, Rev. Palaeobot. and Palyno., 141, 303–312, 2006.
Garzón, G., Alonso, A., Torres, T., and Llamas, J.: Edad de las playas colgadas y de las turberas de Oyambre y Merón (Cantabria), Geogaceta, 20, 498–501, 1996.
Goosse, H. and Fichefet, T.: Importance of ice-ocean interactions for the global ocean circulation: A model study, J. Geophys. Res.-Oceans, 104, 23 337–23 355, 1999.
Heiri, O., Lotter, A. F., Hausmann, S., and Kienast, F.: A chironomid-based Holocene summer air temperature reconstruction from the Swiss Alps, The Holocene, 13, 477–484, 2003.
Indermühle, A., Stocker, T., Joos, F., Fischer, H., Smith, H., Wahlen, M., Deck, B., Mastroianni, D., Tschumi, J., Blunier, T., Meyer, R., and Stauffer, B.: Holocene carbon-cycle dynamics based on CO_2 trapped in ice at Taylor Dome, Antarctica, Nature, 398, 121–126, 1999.
Jessen, C. A., Rundgren, M., Bjorck, S., and Hammarlund, D.: Abrupt climatic changes and an unstable transition into a late Holocene Thermal Decline: a multiproxy lacustrine record from southern Sweden, J. Quat. Sci., 20, 349–362, 2005.
Jessen, C. A., Rundgren, M., Björck, S., and Muscheler, R.: Climate forced atmospheric CO_2 variability in the early Holocene: A stomatal frequency reconstruction, Global Planet. Change, 57, 247–260, 2007.
Kaplan, M. R., and Wolfe, A. P.: Spatial and temporal variability of Holocene temperature in the North Atlantic region, Quat. Res., 65, 223–231, 2006.
Kaufman, D. S., Ager, T. A., Anderson, N. J., Anderson, P. M., Andrews, J. T., Bartlein, P. J., Brubaker, L. B., Coats, L. L., Cwynar, L. C., and Duvall, M. L.: Holocene thermal maximum in the western Arctic (0–180 W), Quat. Sci. Rev., 23, 529–560, 2004.
Kouwenberg, L., Wagner, R., Kürschner, W., and Visscher, H.: Atmospheric CO_2 fluctuations during the last millennium reconstructed by stomatal frequency analysis of Tsuga heterophylla needles, Geology, 33, 33–36, 2005.
Kouwenberg, L. L. R., McElwain, J. C., Kürschner, W. M., Wagner, F., Beerling, D. J., Mayle, F. E., and Visscher, H.: Stomatal frequency adjustment of four conifer species to historical

changes in atmospheric CO_2, Am. J. Bot., 90, 610–619, 2003.
Kürschner, W.: Leaf stomata as boisensors of palaeoatmosferic CO_2 levels, LPP contributions series 5, Utrecht University, The Netherlands, 153 pp., 1996.
Kürschner, W.: The anatomical diversity of recent and fossil leaves of the durmast oak (*Quercus petraea* Lieblein/Q. *pseudocastanea* Goeppert) – implications for their use as biosensors of palaeoatmospheric CO_2 levels, Rev. Palaeobot. Palyno., 96, 1–30, 1997.
Liu, Z., Brady, E., and Lynch-Stieglitz, J.: Global ocean response to orbital forcing in the Holocene, Paleoceanogr., 18, 1041, 2003.
Lockheart, M., Poole, I., van Bergen, P., and Evershed, R.: Leaf carbon isotope compositions and stomatal characters: important considerations for palaeoclimate reconstruction, Org. Geochem., 29, 4, 1998.
Marchal, O., Cacho, I., Stocker, T. F., Grimalt, J. O., Calvo, E., Martrat, B., Shackleton, N., Vautravers, M., Cortijo, E., and van Kreveld, S.: Apparent long-term cooling of the sea surface in the northeast Atlantic and Mediterranean during the Holocene, Quat. Sci. Rev., 21, 455–483, 2002.
McElwain, J. C., Mayle, F. E., and Beerling, D. J.: Stomatal evidence for a decline in atmospheric CO_2 concentration during the Younger Dryas stadial: a comparison with Antarctic ice core records, J. Quat. Sci., 17, 21–29, 2002.
Monnin, E., Steig, E. J., Siegenthaler, U., Kawamura, K., Schwander, J., Stauffer, B., Stocker, T. F., Morse, D. L., Barnola, J. M., and Bellier, B.: Evidence for substantial accumulation rate variability in Antarctica during the Holocene, through synchronization of CO_2 in the Taylor Dome, Dome C and DML ice cores, Earth Planet. Sc. Lett., 224, 45–54, 2004.
Myhre, G., Highwood, E. J., Shine, K. P., and Stordal, F.: New estimates of radiative forcing due to well mixed greenhouse gases, Geophys. Res. Lett., 25, 2715–2718, 1998.
Ojala, A. E. K., Alenius, T., Seppä, H., and Giesecke, T.: Integrated varve and pollen-based temperature reconstruction from Finland: evidence for Holocene seasonal temperature patterns at high latitudes, The Holocene, 18, 529, 2008.
Opsteegh, J. D., Haarsma, R. J., Selten, F. M., and Kattenberg, A.: A dynamic alternative to mixed boundary conditions in ocean models, Tellus A, 50, 348–367, 1998.
Pagés, J., Alonso, A., Cearreta, A., Hacar, M., and Bao, R.: The Holocene record in the Villaviciosa estuary (Asturias, Spain), in: Quaternary climatic changes and environmental crisis in the Mediterranean Region, edited by: edited by: Ruiz Zapata, M.B., Dorado Valiño, M., Valdeolmillos Rodríguez, A., Gil García, M. J., Bardají Azcárate, T., Bustamante Gutiérrez,

I., and Martínez Mendizábal, I., Universidad de Alcalá-MCYT-INQUA, Alcalá de Henares, Madrid, Spain, 249–256, 2003.
Peñalba, M., Arnold, M., Guiot, J., Duplessy, J.-C., and de Beaulieu, J.: Termination of the last glaciation in the Iberian peninsula inferred from the pollen sequence of Quintanar de la Sierra, Quat. Res., 48, 205–214, 1997.
Peñas, A., Llamas, F., Pérez Morales, C., and Acedo, C.: Aportaciones al conocimiento del género Quercus en la cordillera Cantábrica – I: Tricomas Foliares de las especies caducifolias, Lagascalia, 17, 311–324, 1994.
Petit, J., Jouzel, J., Raynaud, D., Barkov, N., Barnola, J., Basile, I., Bender, M., Chappellaz, J., Davisk, M., Delaygue, G., Delmotte, M., Kotlyakov, V., Legrand, M., Lipenkov, V., Lorius, C., Pépin, L., Ritz, C., Saltzmank, E., and Stievenard, M.: Climate and atmospheric history of the past 420 000 years from the Vostok ice core, Antarctica, Nature, 399, 429–436, 1999.
Poole, I., Weyers, J., Lawson, T., and Raven, J.: Variations in stomatal density and index: implications for palaeoclimatic reconstructions, Plant, Cell Environ., 19, 705–712, 1996.
Raynaud, D., Jouzel, J., Barnola, J., Chappellaz, J., Delmas, R., and Lorius, C.: The ice record of greenhouse gases, Science, 259, 926–934, 1993.
Reimer, P., Baillie, M., Bard, E., Bayliss, A., Beck, J., Bertrand, C., Blackwell, P., Buck, C. B., G, Cutler, K., Damon, P., Edwards, R., Fairbanks, R., Friedrich, M., Guilderson, T., Hughen, K., Kromer, B., McCormac, F., Manning, S., Bronk Ramsey, C., Reimer, R., Remmele, S., Southon, J., Stuiver, M., Talamo, S., Taylor, F., van der Plicht, J., and Weyhenmeyer, C.: IntCal04 Terrestrial radiocarbon age calibration, 26–0 ka BP, Radiocarbon, 46, 1029–1058, 2004.
Rundgren, M. and Beerling, D.: A Holocene CO_2 record from stomatal index of subfossil *Salix herbacea* L. leaves from northern Sweden, The Holocene, 9,5, 509–513, 1999.
Rundgren, M. and Björck, S.: Late-glacial and early Holocene variations in atmospheric CO_2 concentration indicated by high-resolution stomatal index data, Earth Planet. Sc. Lett., 213, 19–204, 2003.
Seppä, H., Hammarlund, D., and Antonsson, K.: Low-frequency and high-frequency changes in temperature and effective humidity during the Holocene in south-central Sweden: implications for atmospheric and oceanic forcings of climate, Clim. Dynam., 25, 285–297, 2005.
Shackleton, N.: The 100 000-year ice-age cycle identified and found to lag temperature, carbon dioxide, and orbital eccentricity, Science, 289, 1897–1902, 2000.
Stott, P. and Kettleborough, J.: Origins and estimates of uncertainty in predictions of twenty-first

century temperature rise, Nature, 416, 723–726, 2002.
Trudinger, C. M., Rayner, P. J., Enting, I. G., Heimann, M., and Scholze, M.: Implications of ice core smoothing for inferring CO_2 flux variability, J. Geophys. Res., 108, 4492, doi:10.1029/2003JD003562, 2003.
Uzunova, K., Palamarev, E., and Ehrendorfer, F.: Anatomical changes and evolutionary trends in the foliar epidermis of extant and fossil Euro-Mediterranean oaks (Fagaceae), Plant Syst. Evol., 204, 141–159, 1997.
van Hoof, T., Kaspers, K., Wagner, F., de Wal, R., Kürschner, W., and Visscher, H.: Atmospheric CO_2 during the 13th century AD: reconciliation of data from ice core measurements and stomatal frequency analysis, Tellus B, 57, 351–355, 2005.
Wagner, F., Bohncke, S., Dilcher, D., Kürschner, W., van Geel, B., and Visscher, H.: Century-scale shifts in early Holocene atmospheric CO_2 concentration, Science, 284, 1971–1973, 1999.
Wagner, F., Aaby, B., and Visscher, H.: Rapid atmospheric CO_2 changes associated with the 8200-years-B.P. cooling event, P. Ntl. Acad. Sci. USA, 99, 12 011–12 014, 2002.
Wagner, F., Kouwenberg, L., van Hoof, T., and Visscher, H.: Reproducibility of Holocene atmospheric CO_2 records based on stomatal frequency, Quat. Sci. Rev., 23, 1947–1954, 2004.
Westerkamp, C. and Demmelmeyer, H.: Leaf surfaces of Central European woody plants, Atlas and keys, Gebrüder Borntraeger, Berlin and Stuttgart, Germany, 558 pp., 1997.

Table 1. Sampled sites list.

Sites	Location (UTM)			Samples	Depth	^{14}C dates	Calendar dates	Beta code	CO_2
	Zone	X	Y		(m)	(BP)	(2σ cal BP)		(ppmv) ($\pm 1\sigma$)
Pravia	29	736 087	4 822 585	PR 6/22	22	8300±90	9250±150	208 813	324.09±11.1
				PR 6/18	18	8320±60	9300±170	23 1046	322.20±7.61
				PR 12/8	8–13	6500±60	7420±130	208 814	327.13±5.84
Villaviciosa	30	304 006	4 819 233	At	3	1230±70	1130±220	154 347	332.82±10
				Ab	6	3750±40	4110±130	231 045	325.65±13.7
				B (VIL.10)	8	3620±50	3950±140	179 600	332.72±2.88
				D (VIL.D.O)	10	4750±70	5450±190	9094	336.75±7.61
				E (VIL.E1)	15	5130±60	5860±140	179 601	341.60±13.8
Merón	30	389 456	4 805 983	M1B	1	5920±70	6750±140	111 250	337.85±6.43

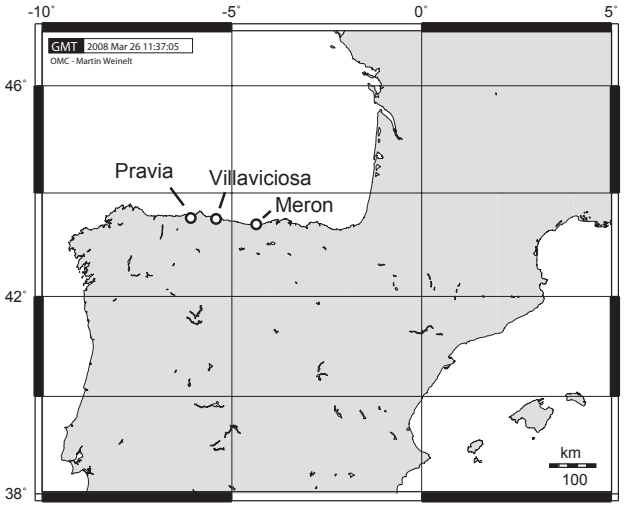

Fig. 1. Location of sampled sites (Weilnet, 1996–2006, http://www.aquarius.ifm-geomar.de/).

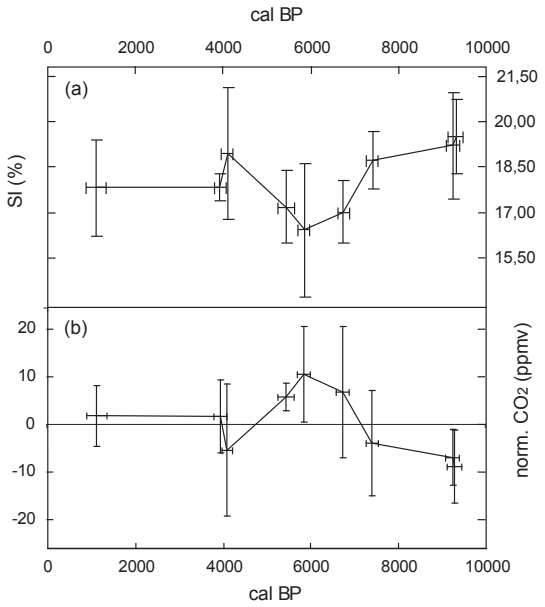

Fig. 2. (a) Mean stomatal index (SI %) values (dots) of fossil layers based on stomatal counts. **(b)** Reconstructed normalized CO_2 mixing ratios (ppmv) for 9250–1130 cal PB, based on the *Q. robur* SI record and the CO_2 inference model for northern Iberia [CO_2[ppmv]=−6.25×(SI −71.09); Garcia-Amorena et al., 2006]. Error bars: ±1 standard deviation for SI, reconstructed CO_2 and cal BP.

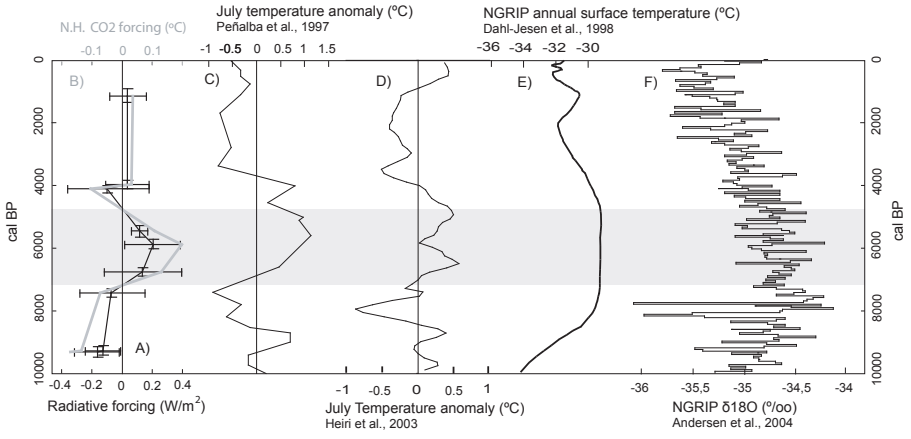

Fig. 3. Comparison of **(a)** variations in radiative forcing (W/m^2) (±1×standard deviation) inferred from the reconstructed normalised atmospheric CO_2 concentrations, **(b)** temperature changes (˚C) in the Northern Hemisphere based on the radiative forcing variation induced by the CO_2 mixing radios changes, **(c)** reconstructed July temperature anomalies (˚C) for the Iberian Range (Quintanar de la Sierra; 1470 m a.s.l.) based on pollen analysis, **(d)** chironomid-based July temperature anomalies (˚C) in the northern Swiss Alps (Hinterburgsee; 1515 m a.s.l.), **(e)** reconstructed North GRIP surface temperature (˚C) (Dahl-Jensen et al., 1998) **(f)** North GRIP δ^{18}O (‰) (Andersen et al., 2004).